Nature Communications

https://doi.org/10.1038/s41467-026-69968-y

Article in Press

Engineering LmrR protein for L-proline-based asymmetric aldol biocatalysis

Received: 9 July 2025

Accepted: 13 February 2026

Cite this article as: Lu, H., Liu, W.-Q., Ji, X. *et al.* Engineering LmrR protein for L-proline-based asymmetric aldol biocatalysis. *Nat Commun* (2026). https://doi.org/10.1038/s41467-026-69968-y

Haofan Lu, Wan-Qiu Liu, Xiangyang Ji, Xiao Zheng, Yuhao Zhang, Yuhao Luo, Yiyao Guo & Jian Li

Engineering LmrR protein for L-proline-based asymmetric aldol biocatalysis

Haofan Lu[1], Wan-Qiu Liu[1], Xiangyang Ji[1], Xiao Zheng[1], Yuhao Zhang[1], Yuhao Luo[1], Yiyao Guo[1] & Jian Li[1,2,3*]

[1]School of Physical Science and Technology, ShanghaiTech University, Shanghai, China

[2]State Key Laboratory of Advanced Medical Materials and Devices, ShanghaiTech University, Shanghai, China

[3]Shanghai Clinical Research and Trial Center, Shanghai, China

*Corresponding author.

E-mail: lijian@shanghaitech.edu.cn (J.L.).

Abstract

L-Proline is a powerful organocatalyst widely applied in asymmetric synthesis due to its secondary amine functionality. However, in proteins, this functional group is locked in peptide bonds, rendering proline catalytically inactive. Natural enzymes that leverage L-proline-based catalysis are exceedingly rare. Here, we engineer the nonenzymatic protein scaffold LmrR into a new-to-nature biocatalyst by exposing its native L-proline residue at the *N*-terminus to catalyze enantioselective aldol reactions. Through rational design, protein engineering, and reaction optimization, we develop an engineered LmrR variant that achieves up to 99% conversion and >99% enantiomeric excess across a range of aromatic and heteroaromatic aldehyde substrates. Our findings reveal a unique strategy for unlocking dormant catalytic potential in natural amino acids and protein scaffolds, providing an applicable approach to create tailored, L-proline-based enzymes for asymmetric synthesis.

Introduction

Enzymes offer green and sustainable solutions for synthetic chemistry due to their high enantioselectivity, rapid reaction rates, and operation under environmentally benign conditions[1-3]. Consequently, they have been widely employed in the synthesis of various valuable molecules from pharmaceutical building blocks to complex natural products[4-6]. However, natural enzymes are inherently constrained by their evolved biological functions, which often fall short of meeting the diverse and growing demands of industrial and pharmaceutical synthesis. To overcome these limitations, extensive efforts have focused on enzyme engineering[7,8], directed evolution[9,10], and chemical modification[11,12] to enhance catalytic selectivity, efficiency, and substrate scope.

The design and evolution of artificial enzymes have emerged as powerful strategies to expand the catalytic capabilities of proteins beyond those found in nature[13,14]. Several nonenzymatic protein scaffolds (e.g., streptavidin, serum albumins, and multidrug resistance regulators) have been repurposed through the incorporation of noncanonical catalytic elements, resulting in artificial enzymes with novel reactivities, improved stability, and enhanced catalytic efficiency[15-17]. Among these, the bacterial transcriptional regulator LmrR from *Lactococcus lactis* has attracted attention as a versatile scaffold due to its large hydrophobic pocket at the dimer interface, which facilitates substrate binding[18,19]. The Roelfes group and others have extensively engineered LmrR into functional biocatalysts, including metalloenzymes and photoenzymes, for a range of abiological chemical transformations[20-27]. Notably, a boronic acid-dependent LmrR-based enzyme was developed to catalyze enantioselective organocatalytic reactions inaccessible to natural enzymes[25]. In another example, a synthetic triplet photosensitizer was incorporated into LmrR to enable photoenzymatic energy transfer cycloadditions[24]. These advances underscore the versatility and evolvability of LmrR. However, such designs typically rely on genetic code expansion—incorporating noncanonical amino acids via amber suppression—to create functional catalytic sites[20-27]. This technique remains limited by the availability of orthogonal translation systems, high costs of noncanonical amino acids, misincorporation, and reduced protein expression yields[16]. To date, no artificial enzyme based on LmrR has utilized only native residues as catalytic sites.

L-Proline and its derivatives are widely used in asymmetric organic synthesis, enabling key transformations such as aldol reactions[28,29], Michael additions[30,31], and Mannich reactions[32,33], among others[34-37]. The catalytic activity of L-proline arises from its secondary amine, which forms an enamine intermediate with carbonyl substrates[36]. However, in proteins, this functional group is typically inactivated by peptide bond formation, making proline-based catalysis extremely rare in nature. One of the few known exceptions is 4-oxalocrotonate tautomerase (4-OT), which possesses an *N*-terminal L-proline that mediates secondary amine catalysis and has been engineered for asymmetric reactions[38-44]. Inspired by this precedent, we aim

to exploit the *N*-terminal L-proline of LmrR as a native catalytic element, avoiding the need for noncanonical amino acids or synthetic cofactors.

Here, we engineer the nonenzymatic transcriptional regulator LmrR into a natural aldolase-like enzyme by exposing its native L-proline residue at the *N*-terminus to serve as an organocatalyst (**Fig. 1**). To achieve this, we reposition the proline residue in LmrR from position five to the *N*-terminus, thereby liberating its secondary amine within the hydrophobic pocket to enable enantioselective aldol catalysis. Specifically, we modify the LmrR sequence by removing the first four residues and subsequently deleting three additional residues to shift the exposed *N*-terminal L-proline deeper into the hydrophobic pocket (**Fig. 1b**). Through rational design and reaction optimization, we obtain an LmrR variant that mimics natural aldolase activity, exhibiting high catalytic efficiency in asymmetric aldol reactions with substrate conversions up to 99% and enantiomeric excess (*e.e.*) values over 99% (**Fig. 1c**). This work presents a rational strategy for designing new-to-nature biocatalysts from the nonenzymatic protein scaffold (LmrR). While demonstrated successfully with LmrR, this enzyme design strategy depends on the presence and position of proline residues within the scaffold protein. In cases where a suitable proline is absent, a proline residue could be directly introduced at the *N*-terminus and subsequently repositioned into a hydrophobic cavity to achieve catalysis and stereoselective chemical transformations.

Results

Discovery of LmrR-catalyzed aldol reaction

LmrR has been widely employed as a privileged scaffold for the design of artificial enzymes, owing to its large hydrophobic pocket that can accommodate a broad range of substrates[20-27]. Although LmrR lacks any known native enzymatic function[14,19,25], its hydrophobic pocket alone may nonetheless support latent catalytic activity. To probe this possibility, we selected a model asymmetric aldol reaction between cyclohexanone and 4-nitrobenzaldehyde and evaluated its efficiency in the presence of LmrR (**Fig. 2a**). Remarkably, LmrR (1.5 mol%) catalyzed the reaction with 95% conversion (based on 20 mM 4-nitrobenzaldehyde), albeit with low enantioselectivity (7% *e.e.*) (**Fig. 2b**). For comparison, we assessed L-proline (1.5 mol%) under the same conditions. Yet, no product formation was observed in either aqueous or organic media (**Fig. 2b**), consistent with the requirement for high catalyst loadings (typically up to 30 mol%) in conventional proline-catalyzed aldol reactions[28] (**Fig. 1a**). These results suggest that LmrR provides a catalytic advantage over free L-proline, likely due to substrate preorganization within its hydrophobic pocket, and highlight the potential of native LmrR as a starting point for enzyme-like aldol catalysis.

Encouraged by this unexpected catalytic activity, we next investigated which residues might contribute to the native aldolase-like activity of LmrR. Sequence analysis revealed that LmrR contains nine lysine

residues (**Fig. 1b**; see the full sequence in **Supplementary Information**). Given that lysine's ε-amino group (primary amine) is essential for catalysis in class I aldolases[45-48], we hypothesized that these residues could be mediating the observed aldol reaction. To verify this hypothesis, we first mutated three lysine residues (K6, K22, and K101), located near the hydrophobic pocket, to alanine, generating the LmEK variant (**Fig. 1b**). This mutation significantly reduced the conversion to ~10%. However, further mutating the remaining six lysine residues to alanine (yielding LmrR_No Lys; with K77 substituted by glutamine to improve solubility) resulted in only a slightly additional decrease in activity (~8% conversion) **(Fig. 2b**). To further rule out contributions from primary amine groups at the protein surface or *N*-terminus, we chemically blocked all primary amines using a *t*-butyloxycarbonyl (Boc) protecting group. The Boc-modified LmrR and LmrR_No Lys showed similar conversion rates to LmEK, without further reduction (**Fig. 2b**). Together, these results suggest that the three lysine residues (K6, K22, and K101) proximal to the active site primarily account for LmrR's intrinsic catalytic activity.

To further validate the role of the three lysine residues in catalysis, we conducted reductive amination-based trapping experiments to probe their interaction with the aldol substrates. Specifically, parental LmrR and its lysine-to-alanine mutant (LmEK) were incubated with cyclohexanone, 4-nitrobenzaldehyde, and sodium triacetoxyborohydride [$NaBH(OAc)_3$], a mild reductant that irreversibly traps transient enamine intermediates via covalent bond formation (**Fig. 2c**). Following incubation, matrix-assisted laser desorption/ionization time-of-flight mass spectrometry (MALDI-TOF-MS) analysis revealed a mass shift in parental LmrR consistent with three covalent modifications—corresponding to the addition of three cyclohexane-derived groups (**Fig. 2d**, top). In contrast, no such modification was observed in the LmEK variant (**Fig. 2d**, bottom), confirming the involvement of K6, K22, and K101 in forming the enamine intermediate. These data demonstrate that the three lysine residues proximal to the hydrophobic pocket provide nucleophilic primary amines essential for the observed aldol reactivity of LmrR, achieving up to 95% substrate conversion (**Fig. 2b**). We next evaluated LmrR variants retaining one or two lysine residues in the hydrophobic pocket. All such variants showed high conversions (93-96%) but low enantioselectivities (6-11% *e.e.*) (**Supplementary Fig. 1**). These findings indicate that although lysine residues (K6, K22, K101) can serve as catalytic nucleophiles, the LmrR pocket does not provide the chiral environment necessary for effective stereocontrol. While natural lysine-dependent aldolases achieve high enantioselectivity through highly organized active sites[48-50], engineering LmrR to create a similarly preorganized chiral pocket around lysine would require extensive structural redesign. Therefore, in this work we pursued an alternative and complementary strategy, leveraging proline-mediated enamine catalysis to introduce a chiral catalytic element directly into the active site.

Rational design of LmrR for high enantioselectivity

With the LmrR variant LmEK (**Fig. 1b**) in hand, we aimed to enhance its enantioselectivity through rational design and protein engineering (**Fig. 3a**). Our approach consisted of three main strategies. First, leveraging

the broad catalytic versatility of L-proline's secondary amine[28-37], we repositioned the native proline residue at position 5 to the *N*-terminus of LmEK by deleting the initial four residues (G1–I4), thereby exposing the proline as a free *N*-terminal organocatalyst. This design mimics the rare natural enzyme 4-oxalocrotonate tautomerase (4-OT), which features an *N*-terminal L-proline as its catalytic center[38-44]. Second, to optimize substrate binding, we further truncated residues following the *N*-terminal proline to relocate it closer to the hydrophobic pocket's core, where two central tryptophan residues (W96 and W96' in native LmrR) provide π–π interactions to recruit aromatic substrates[19,20,24]. Third, we applied targeted mutagenesis to polar residues surrounding the proline in the pocket, aiming to reduce unfavorable hydrogen bonding with the substrates that might hinder effective catalysis. Based on precedent from 4-OT[38,51] and classical proline organocatalysis[52-54], we propose that our engineered LmrR catalyzes the aldol reaction via an enamine intermediate formed between the secondary amine of the *N*-terminal proline and cyclohexanone (**Fig. 3b**), facilitating nucleophilic addition to the aldehyde.

To initiate our design, we deleted the first four residues (G1–I4) from both LmEK and parental LmrR, generating the variants LPEK1 and LNP, respectively. Since these proteins were expressed in *E. coli*, endogenous methionine aminopeptidase catalyzed the cleavage of the *N*-terminal methionine from the nascent polypeptides[55-57], thereby exposing the L-proline residue at position 1. The successful removal of the *N*-terminal methionine in all variants was confirmed by MALDI-TOF-MS, which showed excellent agreement between the observed and calculated molecular weights (**Fig. 3c**). To confirm that the exposed *N*-terminal L-proline mediated the proposed enamine catalysis (**Fig. 3b**), we repeated the reductive trapping experiments by incubating the variants with the substrates and $NaBH(OAc)_3$. Notably, the LNP variant derived from parental LmrR exhibited a major mass peak corresponding to four cyclohexane modifications (**Fig. 3c**), indicating that the *N*-terminal proline trapped one substrate molecule in addition to the three lysine residues (K6, K22, and K101) previously identified (**Fig. 2d**, top panel). Upon mutation of these three lysines to alanine, all four LPEK variants showed only a single modification peak, consistent with trapping exclusively by the *N*-terminal L-proline residue (**Fig. 3c** and **Supplementary Fig. 2**). Collectively, these results confirm that in our engineered LPEK variants, the *N*-terminal L-proline functions as the sole organocatalyst mediating enamine-based catalysis.

Next, we evaluated the catalytic performance of various LmrR variants. Notably, all variants, including parental LmrR, exhibited similarly high conversions ranging from 88% to 96% (**Fig. 3d**), demonstrating the robustness of these enzymes for this transformation. However, their enantioselectivities varied significantly (**Fig. 3e**). Exposing the L-proline residue at the *N*-terminus (variant LNP) resulted in a more than threefold increase in enantioselectivity compared to parental LmrR, highlighting the pivotal role of L-proline in asymmetric catalysis. Further improvement was observed in LPEK1, where mutation of the three lysine residues (K6, K22, and K101) in the hydrophobic pocket enhanced enantioselectivity. Building on this, starting from LPEK1—which exhibited moderate enantioselectivity (34% *e.e.*; **Fig. 3e**)—we conducted three

rounds of protein engineering to further boost enantioselectivity (**Fig. 1b**). In the first round, we sought to reposition the *N*-terminal proline (P1) closer to the center of the hydrophobic pocket by deleting one, two, or three residues following P1 (**Fig. 3a**, bottom). Deleting all three residues (A2, E3, and M4) to generate the LPEK2 variant led to an approximately 40% increase in enantioselectivity relative to LPEK1 (**Fig. 3e**). Structural comparisons revealed that the distance between P1 and residue W89' (formerly W96' in parental LmrR) was shorter in LPEK2 than in LPEK1 (**Supplementary Fig. 3**), consistent with our hypothesis that shifting P1 closer to the pocket center enhances enantiocontrol.

Based on LPEK2, we initiated the second round of protein engineering by targeting residues near P1, specifically polar amino acids Q5, R49, S88, S90, and D93, for mutation. These residues were substituted with nonpolar amino acids of similar steric bulk (**Fig. 1b**), aiming to disrupt hydrogen bonding with the substrate and thereby enhance enantioface discrimination. Among the resulting variants, LPEK2_S88A (designated LPEK3) exhibited the most significant improvement, achieving an enantioselectivity of 66% *e.e.* (**Fig. 3e**). Molecular docking suggests this improvement arises from the elimination of a hydrogen bond between the hydroxyl group (-OH) of S88 and the nitro group ($-NO_2$) of 4-nitrobenzaldehyde (**Supplementary Fig. 4a**). Recognizing the critical role of residue S88 in enantioselectivity, we performed saturation mutagenesis at this position. While several S88 mutants showed enhanced enantioselectivity compared to LPEK2, none surpassed the performance of LPEK3 (LPEK2_S88A; **Supplementary Fig. 4b**).

In the third round, we aimed to increase the flexibility of P1 within the hydrophobic pocket by disrupting the *N*-terminal rigid α-helix. To achieve this, we targeted residues R3 and Q5 for mutation to glycine (G) and/or proline (P). Glycine's small side chain confers high flexibility, while proline's unique cyclic structure disrupts α-helix formation by preventing hydrogen bonding. Using LPEK3 as the parent, we generated variants and evaluated their catalytic performance. Among them, the variant LPEK3_R3P_Q5G (designated LPEK4) showed the highest enantioselectivity, reaching 73% *e.e.* (**Fig. 3e**). These results highlight the advantage of introducing localized structural disorder to increase flexibility (**Supplementary Fig. 5**), a factor that may be beneficial for enhancing protein functions such as enantioselectivity in our designer enzymes. To examine whether an *N*-terminal primary amine could also mediate stereoselective catalysis, we constructed LPEK4_P1A, in which the *N*-terminal proline was replaced with alanine. Although LPEK4_P1A retained high catalytic activity (92% conversion), its enantioselectivity remained low (11% *e.e.*) (**Supplementary Fig. 6**). These results indicate that the *N*-terminal secondary amine of proline is essential for stereocontrol in the LPEK variants. Taken together, through rational design and protein engineering, we improved the enantioselectivity of the designer enzyme LPEK4 (73% *e.e.*) to more than tenfold that of the initial parental LmrR (7% *e.e.*).

Finally, we characterized the structure and kinetics of the optimized variant LPEK4. We employed AlphaFold prediction, circular dichroism (CD) spectroscopy, size exclusion chromatography (SEC), and transmission

electron microscopy (TEM) to assess structural integrity. Our analyses showed that all variants maintained well-preserved structures with characteristics consistent with parental LmrR (**Supplementary Figs. 7-10**). Despite the deletion of a short *N*-terminal fragment comprising seven residues, each variant retained its hydrophobic pocket, supporting high catalytic activity and substrate conversion (**Fig. 3d**). We also measured kinetic parameters (k_{cat} and K_m) for LPEK4 and LmrR (**Supplementary Fig. 11**). Although the catalytic efficiency of LPEK4 (k_{cat}/K_m = 1.14 × 10^{-2} mM^{-1} s^{-1}) was lower than that of LmrR (k_{cat}/K_m = 2.59 × 10^{-2} mM^{-1} s^{-1}), LPEK4 exhibited a markedly improved enantioselectivity compared to the parental enzyme (**Fig. 3e**). In addition, we measured the kinetic parameters of three LmrR variants (LmEK_A6K, LmEK_A22K, and LmEK_A101K), each retaining only a single lysine residue in the active site (**Supplementary Fig. 12**). These variants also exhibited substantially reduced catalytic efficiencies (0.59-0.86 x 10^{-2} mM^{-1} s^{-1}) compared to LmrR containing three lysine residues. Together with the kinetic data for LPEK4, these observations suggest that the reduced catalytic efficiency arises primarily from the reduced number of catalytically active residues in the pocket, rather than from the nature of the *N*-terminal proline itself. Yet importantly, this reduction in activity is accompanied by a substantial gain in enantioselectivity, highlighting the trade-off between turnover and stereochemical control.

Optimization of LPEK4-based catalysis

Using the optimal LPEK4 variant, we next optimized the reaction conditions for the asymmetric aldol addition, focusing on two key parameters (reaction temperature and pH) that influence catalytic activity and enantioselectivity of enzymes[58-61]. We first varied the reaction temperature from 10 to 30 °C in PBS buffer (pH 7.3) with 1.5 mol% biocatalyst. The results indicated that the lowest temperature (10 °C) favored enantioselectivity, achieving 81% *e.e.* compared to 71% *e.e.* at 30 °C, although the substrate conversion was reduced at the lower temperature (**Fig. 4a**). This trend aligns with previous studies showing that temperature can modulate enzyme enantioselectivity[58-60].

Next, we fixed the temperature at 10 °C and examined the effect of pH on LPEK4 performance. Because the conversion after 24 h at 10 °C was relatively low (63%), we extended the reaction time to 48 h. Under these conditions, conversion exceeded 95% at pH values above 5.8 (**Fig. 4b**), but decreased to about 60% at more acidic pH levels of 5.0 and 3.0. Notably, the highest enantioselectivity (90% *e.e.*) was observed at pH 5.8. Overall, a mildly acidic environment (pH 5.0-6.6) enhanced enantioselectivity (85-90% *e.e.*) compared to more acidic or neutral pH conditions (**Fig. 4b**). In addition, the pK_a of the P1 residue in LPEK4 was experimentally determined to be 5.6 (**Supplementary Fig. 13**), consistent with its predicted value (pK_a 5.5) obtained using H++[62,63]. At the reaction pH (5.8), P1 is therefore predominantly in the deprotonated form, facilitating enamine formation. By comparison, P1 in LPEK1 has a higher predicted pK_a (7.0), indicating that repositioning P1 into the hydrophobic pocket of LPEK4 is essential for lowering its pK_a and achieving effective catalysis. Taken together, the optimal conditions for LPEK4-catalyzed asymmetric aldol

addition were determined to be 10 °C, pH 5.8, and a reaction time of 48 h, resulting in up to 95% conversion and 90% enantioselectivity.

Substrate scope of LPEK4

Finally, we investigated the substrate tolerance of our designer enzyme LPEK4 by catalyzing cyclohexanone (**1**) with various 4-nitrobenzaldehyde analogs (**2a-l**) bearing different substituents on the phenyl or heteroaromatic ring (**Fig. 4c**). All reactions were performed under the optimized conditions, and substrate conversion (based on aldehyde **2**), *e.e.* value, and diastereomeric ratio (d.r.) were analyzed. The results showed that LPEK4 efficiently tolerated a range of substituents, including NO_2 (**2a-c**), CN (**2d**,**e**), Cl (**2f**,**g**), and COOMe (**2h**,**i**) on the phenyl ring, achieving excellent conversions of 89-99%. Notably, enantioselectivity and diastereoselectivity were highest when the substituents were located at the *para*-position relative to the aldehyde group, followed by those at the *meta*- and *ortho*-positions (**3a-i**). For example, the product **3h**, derived from a *para*-COOMe substituent, was obtained with 93% conversion and excellent levels of enantioselectivity (>99% *e.e.*) and diastereoselectivity (94:6 *d.r.*). This trend likely reflects that *para*-substituents are spatially distant from both the reactive aldehyde and catalytic residues (e.g., the *N*-terminal L-proline), minimizing steric or electronic interference with the secondary amine-mediated asymmetric aldol reaction. Furthermore, when the phenyl ring of **2** was replaced with a pyridine ring (**2j-l**), LPEK4 maintained good catalytic efficiency and selectivity, producing **3j-l** with up to 81% conversion and 91% *e.e.*. Together, these results demonstrate the robustness and broad substrate promiscuity of LPEK4, which is consistent with previous reports on other LmrR-based designer enzymes such as photoenzymes[24], metalloenzymes[27], and boron-dependent biocatalysts[25].

Discussion

We report the successful development of a new-to-nature biocatalyst by engineering the nonenzymatic protein LmrR to harness its native L-proline residue for asymmetric aldol reactions. Through rational design, protein engineering, and reaction optimization, we created an artificial enzyme that achieves high substrate conversions (up to 99%) and excellent enantioselectivity (>99% *e.e.*) across a broad substrate scope. Our work offers several key innovations. First, we construct an artificial L-proline-based enzyme using a natural *N*-terminal L-proline, inspired by the rare natural example of 4-oxalocrotonate tautomerase[38] but implemented in a synthetic context. This expands the repertoire of biocatalysts and establishes a promising strategy for creating organocatalytic enzymes. Second, by leveraging LmrR's endogenous L-proline residue, we introduce a catalytically competent secondary amine without the need for incorporating noncanonical amino acids[64] or chemical modifications[65]—common approaches that often suffer from technical complexity and low protein production[16]. However, this enzyme design strategy is likely limited to protein scaffolds containing a proline residue near the *N*-terminus that can be repositioned into a hydrophobic pocket. Nevertheless, it enables the creation of an intrinsic, genetically encoded organocatalyst without reliance on nonnatural components, offering distinct advantages in evolvability, scalability, and compatibility with

cellular expression systems. Third, we unveil the latent aldolase-like activity of LmrR and dramatically enhance its enantioselectivity through rational protein engineering, highlighting the versatility of the LmrR scaffold. Altogether, our study demonstrates the potential of natural protein scaffolds such as LmrR with engineerable termini adjacent to a hydrophobic cavity for building robust, tunable, and enantioselective biocatalysts. Given the broad utility of L-proline-based organocatalysis[28-37] and the demonstrated effectiveness of natural L-proline-based biocatalysts—most notably 4-oxalocrotonate tautomerase[38-44] in asymmetric synthesis, this platform offers a promising and accessible route toward the design of tailor-made enzymes for applications in pharmaceutical and chemical synthesis.

Methods

Expression and purification of designer enzymes

LmrR and its derived designer enzymes were expressed in *Escherichia coli* BL21 Gold cells transformed with a pET17b-based plasmid encoding the respective gene. Seed cultures were grown overnight at 37 °C in 20 mL of Luria–Bertani (LB) medium. Subsequently, 15 mL of the seed culture was used to inoculate 1 L of fresh LB medium in a 2.5-L flask, followed by incubation at 37 °C. When OD_{600} reached 0.5-0.6, protein expression was induced with 0.5 mM IPTG, and cells were further cultivated at 20 °C for 16 h.

Cells were harvested by centrifugation at 5000 g and 4 °C for 10 min, then washed once with lysis buffer (10 mM Tris-HCl, 200 mM NaCl, pH 7.0). The cell pellets were resuspended in lysis buffer and lysed by sonication (50% amplitude, 10 s on/off for a total of 40 min). The cell lysate was clarified by centrifugation at 21000 g and 4 °C for 20 min. The resulting supernatant was filtered through a 0.45 μm membrane and subjected to purification using a 5-mL Ni-NTA column (GE Healthcare). Eluted proteins were desalted and concentrated using Amicon Ultra-15 centrifugal filters (3 kDa cutoff, Merck) by centrifugation at 4000 g and 4 °C. Protein concentrations were determined by measuring absorbance at 280 nm using a UV-Vis micro-spectrophotometer (Nano-300, Hangzhou Allsheng Instruments, China). Typical protein yields were between 30 and 50 mg/mL. Purified proteins were flash-frozen in liquid nitrogen and stored at −80 °C until use.

General procedure for enzyme-catalyzed reactions

Enzymatic reactions were performed in a total volume of 50 μL in 2 mL microcentrifuge tubes, using purified enzymes and substrates. A standard reaction mixture consisted of 0.3 mM enzyme, 200 mM cyclohexanone, and 20 mM 4-nitrobenzaldehyde in 10 mM PBS buffer (pH 7.3). Reactions were incubated at 30 °C for 12 hours with shaking at 600 rpm (Thermo-Shaker, MSC-300, Hangzhou Allsheng Instruments, China). Upon completion, each reaction was quenched with 450 μL acetonitrile and analyzed by HPLC to determine substrate conversion. For determination of *e.e.* values, products were extracted with a tenfold volume of ethyl acetate and then analyzed by chiral HPLC.

Data availability

All data supporting the findings of this study are available within the article and its Supplementary Information, or available from the corresponding author upon request. Source data are provided with this paper.

References

1. Kissman, E. N. et al. Expanding chemistry through in vitro and in vivo biocatalysis. *Nature* **631**, 37-48 (2024).
2. O'Connell, A. et al. Biocatalysis: landmark discoveries and applications in chemical synthesis. *Chem. Soc. Rev.* **53**, 2828-2850 (2024).
3. Benítez-Mateos, A. I., Roura Padrosa, D. & Paradisi, F. Multistep enzyme cascades as a route towards green and sustainable pharmaceutical syntheses. *Nat. Chem.* **14**, 489-499 (2022).
4. Huffman, M. A. et al. Design of an in vitro biocatalytic cascade for the manufacture of islatravir. *Science* **366**, 1255-1259 (2019).
5. Barra, L. et al. β-NAD as a building block in natural product biosynthesis. *Nature* **600**, 754-758 (2021).
6. Thorpe, T. W. et al. Multifunctional biocatalyst for conjugate reduction and reductive amination. *Nature* **604**, 86-91 (2022).
7. Lister, T. M. et al. Engineered enzymes for enantioselective nucleophilic aromatic substitutions. *Nature* **639**, 375-381 (2025).
8. Crawshaw, R. et al. Engineering an efficient and enantioselective enzyme for the Morita–Baylis–Hillman reaction. *Nat. Chem.* **14**, 313-320 (2022).
9. Jeschek, M. et al. Directed evolution of artificial metalloenzymes for in vivo metathesis. *Nature* **537**, 661-665 (2016).
10. Mao, R. et al. Biocatalytic, enantioenriched primary amination of tertiary C–H bonds. *Nat. Catal.* **7**, 585-592 (2024).
11. Brogan, A. P. S., Bui-Le, L. & Hallett, J. P. Non-aqueous homogenous biocatalytic conversion of polysaccharides in ionic liquids using chemically modified glucosidase. *Nat. Chem.* **10**, 859-865 (2018).
12. Lu, H., Ouyang, J., Liu, W. Q., Wu, C. & Li, J. Enzyme-polymer-conjugate-based Pickering emulsions for cell-free expression and cascade biotransformation. *Angew. Chem. Int. Ed.* **62**, e202312906 (2023).
13. Lovelock, S. L. et al. The road to fully programmable protein catalysis. *Nature* **606**, 49-58 (2022).
14. Brouwer, B. et al. Noncanonical amino acids: bringing new-to-nature functionalities to biocatalysis. *Chem. Rev.* **124**, 10877-10923 (2024).
15. Liang, A. D., Serrano-Plana, J., Peterson, R. L. & Ward, T. R. Artificial metalloenzymes based on the biotin-streptavidin technology: enzymatic cascades and directed evolution. *Acc. Chem. Res.* **52**, 585-595 (2019).

16. Drienovská, I. & Roelfes, G. Expanding the enzyme universe with genetically encoded unnatural amino acids. *Nat. Catal.* **3**, 193-202 (2020).
17. Hanreich, S., Bonandi, E. & Drienovská, I. Design of artificial enzymes: insights into protein scaffolds. *ChemBioChem* **24**, e202200566 (2023).
18. Madoori, P. K., Agustiandari, H., Driessen, A. J. & Thunnissen, A. M. Structure of the transcriptional regulator LmrR and its mechanism of multidrug recognition. *EMBO J.* **28**, 156-166 (2009).
19. Roelfes, G. LmrR: a privileged scaffold for artificial metalloenzymes. *Acc. Chem. Res.* **52**, 545-556 (2019).
20. Drienovská, I., Mayer, C., Dulson, C. & Roelfes, G. A designer enzyme for hydrazone and oxime formation featuring an unnatural catalytic aniline residue. *Nat. Chem.* **10**, 946-952 (2018).
21. Zhou, Z. & Roelfes, G. Synergistic catalysis in an artificial enzyme by simultaneous action of two abiological catalytic sites. *Nat. Catal.* **3**, 289-294 (2020).
22. Leveson-Gower, R. B., Zhou, Z., Drienovská, I. & Roelfes G. Unlocking iminium catalysis in artificial enzymes to create a Friedel-Crafts alkylase. *ACS Catal.* **11**, 6763-6770 (2021).
23. Liu, Y., Ba, F., Liu, W. Q., Wu, C. & Li, J. Plug-and-play functionalization of protein−polymer conjugates for tunable catalysis enabled by genetically encoded “click” chemistry. *ACS Catal.* **12**, 4165-4174 (2022).
24. Sun, N., et al. Enantioselective [2+2]-cycloadditions with triplet photoenzymes. *Nature* **611**, 715-720 (2022).
25. Longwitz, L., Leveson-Gower, R. B., Rozeboom, H. J., Thunnissen, A. W. H. & Roelfes, G. Boron catalysis in a designer enzyme. *Nature* **629**, 824-829 (2024).
26. Mou, S. B., Chen, K. Y., Kunthic, T. & Xiang, Z. Design and evolution of an artificial Friedel-Crafts alkylation enzyme featuring an organoboronic acid residue. *J. Am. Chem. Soc.* **146**, 26676-26686 (2024).
27. Veen, M. J. et al. Artificial gold enzymes using a genetically encoded thiophenol-based noble-metal-binding ligand. *Angew. Chem. Int. Ed.* **64**, e202421912 (2025).
28. List, B., Lerner, R. A. & Barbas, C. F. Proline-catalyzed direct asymmetric aldol reactions. *J. Am. Chem. Soc.* **122**, 2395-2396 (2000).
29. Torii, H., Nakadai, M., Ishihara, K., Saito, S. & Yamamoto, H. Asymmetric direct aldol reaction assisted by water and a proline-derived tetrazole catalyst. *Angew. Chem. Int. Ed.* **43**, 1983-1986 (2004).
30. List, B., Pojarliev, P. & Martin, H. J. Efficient proline-catalyzed Michael additions of unmodified ketones to nitro olefins. *Org. Lett.* **3**, 2423-2425 (2001).
31. Bae, D., Lee, J. W. & Ryu, D. H. Enantio- and diastereoselective Michael addition of cyclic ketones/aldehydes to nitroolefins in water as catalyzed by proline-derived bifunctional organocatalysts. *J. Org. Chem.* **87**, 16532-16541 (2022).
32. List, B. The direct catalytic asymmetric three-component Mannich reaction. *J. Am. Chem. Soc.* **122**, 9336-9337 (2000).

33. Yang, J. W., Chandler, C., Stadler, M., Kampen, D. & List, B. Proline-catalysed Mannich reactions of acetaldehyde. *Nature* **452**, 453-455 (2008).
34. List, B. Proline-catalyzed asymmetric reactions. *Tetrahedron* **58**, 5573-5590 (2002).
35. Notz, W., Tanaka, F. & Barbas, C. F. III Enamine-based organocatalysis with proline and diamines: the development of direct catalytic asymmetric aldol, Mannich, Michael, and Diels−Alder reactions. *Acc. Chem. Res.* **37**, 580-591 (2004).
36. Mukherjee, S., Yang, J. W., Hoffmann, S. & List, B. Asymmetric enamine catalysis. *Chem. Rev.* **107**, 5471-5569 (2007).
37. Gruttadauria, M., Giacalone, F. & Noto, R. Supported proline and proline-derivatives as recyclable organocatalysts. *Chem. Soc. Rev.* **37**, 1666-1688 (2008).
38. Zandvoort, E., Baas, B. J., Quax, W. J. & Poelarends, G. J. Systematic screening for catalytic promiscuity in 4-oxalocrotonate tautomerase: enamine formation and aldolase activity. *ChemBioChem* **12**, 602-609 (2011).
39. Zandvoort, E., Geertsema, E. M., Baas, B. J., Quax, W. J. & Poelarends, G. J. Bridging between organocatalysis and biocatalysis: asymmetric addition of acetaldehyde to *β*-nitrostyrenes catalyzed by a promiscuous proline-based tautomerase. *Angew. Chem. Int. Ed.* **51**, 1240-1243 (2012).
40. Guo, C., Saifuddin, M., Saravanan, T., Sharifi, M. & Poelarends, G. J. Biocatalytic asymmetric Michael additions of nitromethane to *α,β*-unsaturated aldehydes via enzyme-bound iminium ion intermediates. *ACS Catal.* **9**, 4369-4373 (2019).
41. Saifuddin, M. et al. Enantioselective aldol addition of acetaldehyde to aromatic aldehydes catalyzed by proline-based carboligases. *ACS Catal.* **10**, 2522-2527 (2020).
42. Xu, G., Crotti, M., Saravanan, T., Kataja, K. M. & Poelarends G. J. Enantiocomplementary epoxidation reactions catalyzed by an engineered cofactor-independent non-natural peroxygenase. *Angew. Chem. Int. Ed.* **59**, 10374-10378 (2020).
43. Kunzendorf, A., Xu, G., Saifuddin, M., Saravanan, T. & Poelarends, G. J. Biocatalytic asymmetric cyclopropanations via enzyme-bound iminium ion intermediates. *Angew. Chem. Int. Ed.* **60**, 24059-24063 (2021).
44. Xu, G. et al. Gene fusion and directed evolution to break structural symmetry and boost catalysis by an oligomeric C-C bond-forming enzyme. *Angew. Chem. Int. Ed.* **61**, e202113970 (2022).
45. Lorentzen, E., Siebers, B., Hensel, R. & Pohl, E. Mechanism of the Schiff base forming fructose-1,6-bisphosphate aldolase: structural analysis of reaction intermediates. *Biochemistry* **44**, 4222-4229 (2005).
46. Clapés, P. & Garrabou, X. Current trends in asymmetric synthesis with aldolases. *Adv. Synth. Catal.* **353**, 2263-2283 (2011).
47. Hernández, K., Szekrenyi, A. & Clapés, P. Nucleophile promiscuity of natural and engineered aldolases. *ChemBioChem* **19**, 1353-1358 (2018).

48. Kunzendorf, A. et al. Unlocking asymmetric Michael additions in an archetypical class I aldolase by directed evolution. *ACS Catal.* **11**, 13236-13243 (2021).
49. Zhou, H. et al. Engineering 2-deoxy-D-ribose-5-phosphate aldolase for anti- and syn-selective epoxidations of α,β-unsaturated aldehydes. *Angew. Chem. Int. Ed.* **64**, e202503054 (2025).
50. Hélaine, V. et al. Recent advances in the substrate selectivity of aldolases. *ACS Catal.* **12**, 733-761 (2022).
51. Poddar, H., Rahimi, M., Geertsema, E. M., Thunnissen, A. M. & Poelarends, G. J. Evidence for the formation of an enamine species during aldol and Michael-type addition reactions promiscuously catalyzed by 4-oxalocrotonate tautomerase. *ChemBioChem* **16**, 738-741 (2015).
52. List, B. Enamine catalysis is a powerful strategy for the catalytic generation and use of carbanion equivalents. *Acc. Chem. Res.* **37**, 548-557 (2004).
53. Bock, D. A., Lehmann, C. W. & List, B. Crystal structures of proline-derived enamines. *Proc. Natl. Acad. Sci. USA* **107**, 20636-20641 (2010).
54. Schmid, M. B., Zeitler, K. & Gschwind, R. M. The elusive enamine intermediate in proline-catalyzed aldol reactions: NMR detection, formation pathway, and stabilization trends. *Angew. Chem. Int. Ed.* **49**, 4997-5003 (2010).
55. Lowther, W. T. & Matthews, B. W. Structure and function of the methionine aminopeptidases. *Biochim. Biophys. Acta* **1477**, 157-167 (2000).
56. Xiao, Q., Zhang, F., Nacev, B. A., Liu, J. O. & Pei, D. Protein *N*-terminal processing: substrate specificity of *Escherichia coli* and human methionine aminopeptidases. *Biochemistry* **49**, 5588-5599 (2010).
57. Moatsou, D. et al. Self-assembly of temperature-responsive protein-polymer bioconjugates. *Bioconjug. Chem.* **26**, 1890-1899 (2015).
58. Phillips, R. S. Temperature modulation of the stereochemistry of enzymatic catalysis: prospects for exploitation. *Trends Biotechnol.* **14**, 13-16 (1996).
59. Magnusson, A. O., Takwa, M., Hamberg, A. & Hult, K. An *S*-selective lipase was created by rational redesign and the enantioselectivity increased with temperature. *Angew. Chem. Int. Ed.* **44**, 4582-4585 (2005).
60. Röllig, R., Paul, C. E., Duquesne, K., Kara, S. & Alphand, V. Exploring the temperature effect on enantioselectivity of a Baeyer-Villiger biooxidation by the 2,5-DKCMO module: the SLM approach. *ChemBioChem* **23**, e202200293 (2022).
61. Secundo, F. & Phillips, R. S. Effects of pH on enantiospecificity of alcohol dehydrogenases from *Thermoanaerobacter ethanolicus* and horse liver. *Enzyme Microb. Technol.* **19**, 487-492 (1996).
62. Gordon, J. C. et al. H++: a server for estimating pK_as and adding missing hydrogens to macromolecules. *Nucleic Acids Res.* **33**, W368-W371 (2005).
63. Anandakrishnan, R., Aguilar, B. & Onufriev, A. V. H++ 3.0: automating p*K* prediction and the preparation of biomolecular structures for atomistic molecular modeling and simulations. *Nucleic Acids Res.* **40**, W537-W541 (2012).

64. Williams, T. L. et al. Secondary amine catalysis in enzyme design: broadening protein template diversity through genetic code expansion. *Angew. Chem. Int. Ed.* **63**, e202403098 (2024).
65. Zhu, Z., Hu, Q., Fu, Y., Tong, Y. & Zhou, Z. Design and evolution of an enzyme for the asymmetric Michael addition of cyclic ketones to nitroolefins by enamine catalysis. *Angew. Chem. Int. Ed.* **63**, e202404312 (2024).

Acknowledgements

This work was supported by the National Natural Science Foundation of China (grant no. 32571664 to J.L.), the National Key Research and Development Program of China (grant no. 2023YFA0914000 to J.L.), the Shanghai Science and Technology Committee (grant no. 24ZR1451000 to J.L.), and the School of Physical Science and Technology of ShanghaiTech University (grant no. SPST-YSFZ-2024-01 to J.L.). H.L. acknowledges support from the Shanghai Post-doctoral Excellence Program (grant no. 2025520). The authors also acknowledge the High-Performance Computing (HPC) Platform of ShanghaiTech University.

Author contributions

J.L., H.L., and W.-Q.L. designed the experiments. H.L. performed the experiments. X.J. and W.-Q.L. carried out MALDI-TOF-MS analysis. X.Z. performed NMR analysis. Y.Z., Y.L., and Y.G. performed HPLC analysis. H.L. and J.L. analyzed the data and prepared the illustrations. H.L. and J.L. wrote the manuscript with input from all authors. J.L. contributed to project conception and supervised the project.

Competing interests

The authors declare no competing interests.

Figure legends

Fig. 1 Designing and engineering LmrR as an aldolase-like biocatalyst for enantioselective aldol reactions. a, Comparison of enantioselective aldol reactions catalyzed by small-molecule L-proline (organocatalyst) and the engineered LmrR-based enzyme. **b**, Mutagenesis strategies employed for engineering LmrR, including repositioning of the native L-proline and active-site remodeling. **c**, Representative aldol reactions catalyzed by the optimized LmrR variants, showing high conversion and enantioselectivity. The LmrR structure was predicted with AlphaFold.

Fig. 2 Discovery of LmrR-mediated aldol activity. a, Proposed mechanism for lysine-mediated aldol addition between cyclohexanone and 4-nitrobenzaldehyde catalyzed by LmrR. The structure of LmrR was predicted using AlphaFold and subsequently visualized with PyMOL. **b**, Substrate conversions catalyzed by various catalysts. Reactions were conducted in PBS buffer (pH 7.3) with 1.5 mol% catalyst, unless

otherwise noted. -, no catalyst added; *, reaction performed in organic solvent (DMSO). Data are shown as means, with error bars representing the standard deviation from three independent experiments (*n* = 3). **c**, Reductive trapping mechanism for the lysine-catalyzed aldol reaction in LmrR. Upon addition of $NaBH(OAc)_3$, the transient enamine intermediate formed between lysine and cyclohexanone is converted into a stable covalent adduct. **d**, MALDI-TOF-MS analysis of parental LmrR and the lysine-deficient variant LmEK before and after enamine trapping. Top panel: parental LmrR shows three mass shifts corresponding to covalent modifications by cyclohexanone. Bottom panel: LmEK shows no detectable modification, confirming the role of the lysine residues. Source data are provided as a Source Data file.

Fig. 3 Rational design and engineering of LmrR variants for asymmetric aldol catalysis. a, AlphaFold-predicted structures of the variant LmEK (top) and the optimized variant LPEK4 (bottom). **b**, Proposed mechanism of L-proline (secondary amine)-mediated asymmetric aldol catalysis. Upon addition of $NaBH(OAc)_3$, the transient enamine intermediate formed between the *N*-terminal proline and cyclohexanone is covalently trapped, forming an irreversible adduct. **c**, MALDI-TOF-MS analysis of LNP and variants LPEK1-LPEK4 before and after enamine trapping. Additional trapping experiments with other variants are shown in **Supplementary Fig. 2**. **d**, Substrate conversions catalyzed by different LmrR variants. **e**, Enantioselectivity of aldol products catalyzed by different LmrR variants. In **d** and **e**, all reactions were performed in PBS buffer (pH 7.3) with 1.5 mol% biocatalyst. Data are shown as means, with error bars representing the standard deviation from three independent experiments (*n* = 3). Source data are provided as a Source Data file.

Fig. 4 Reaction optimization and substrate scope of LPEK4. a, Effect of reaction temperature on the enantioselective aldol reaction catalyzed by LPEK4. **b**, Effect of pH on catalytic performance. **c**, Substrate scope of the LPEK4-catalyzed asymmetric aldol reaction. Standard reaction conditions: cyclohexanone (**1**, 200 mM), aldehyde substrate (**2**, 20 mM), LPEK4 (1.5 mol%), PBS buffer (10 mM, pH 5.8), 10 °C, and 48 h. Results from reactions catalyzed by LmrR are shown in **Supplementary Fig. 14** for comparison. Data are shown as means, with error bars representing the standard deviation from three independent experiments (*n* = 3). Source data are provided as a Source Data file.

Editor Summary:
L-Proline is a powerful organocatalyst widely applied in asymmetric synthesis due to its secondary amine functionality, however, in proteins, this functional group is locked in peptide bonds, rendering proline catalytically inactive. Here, the authors engineer the nonenzymatic protein scaffold LmrR into a new-tonature biocatalyst by exposing its native L-proline residue at the N-terminus to catalyse enantioselective aldol reactions.

Peer Review Information:
Nature Communications thanks anonymous reviewers for their contribution to the peer review of this work. [A peer review file is available.]

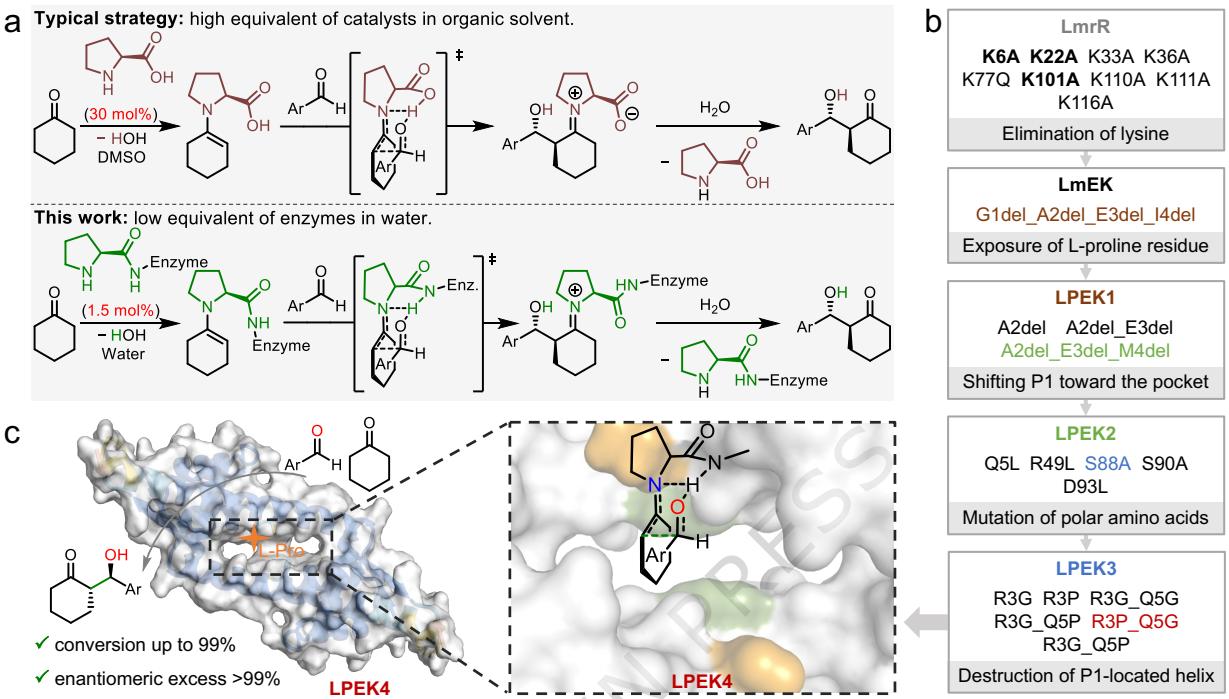

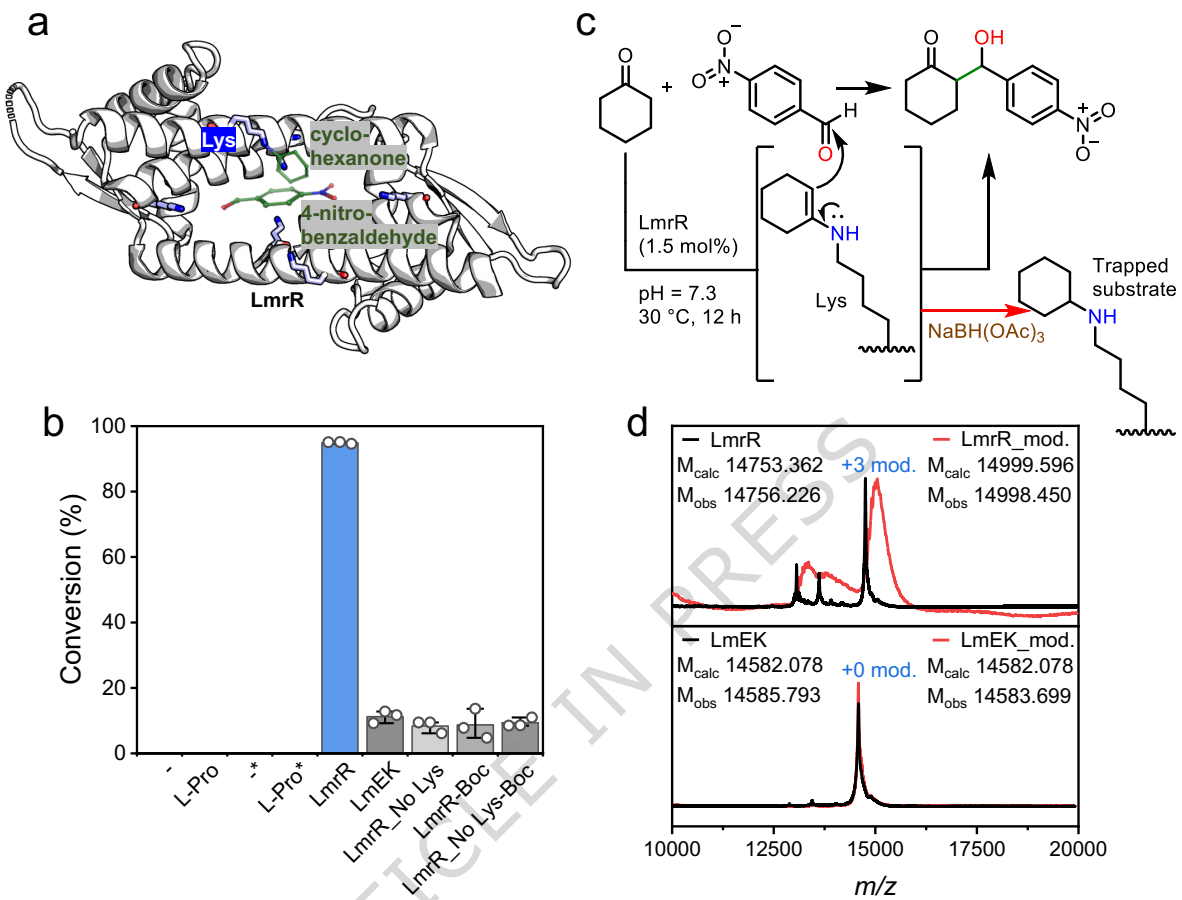

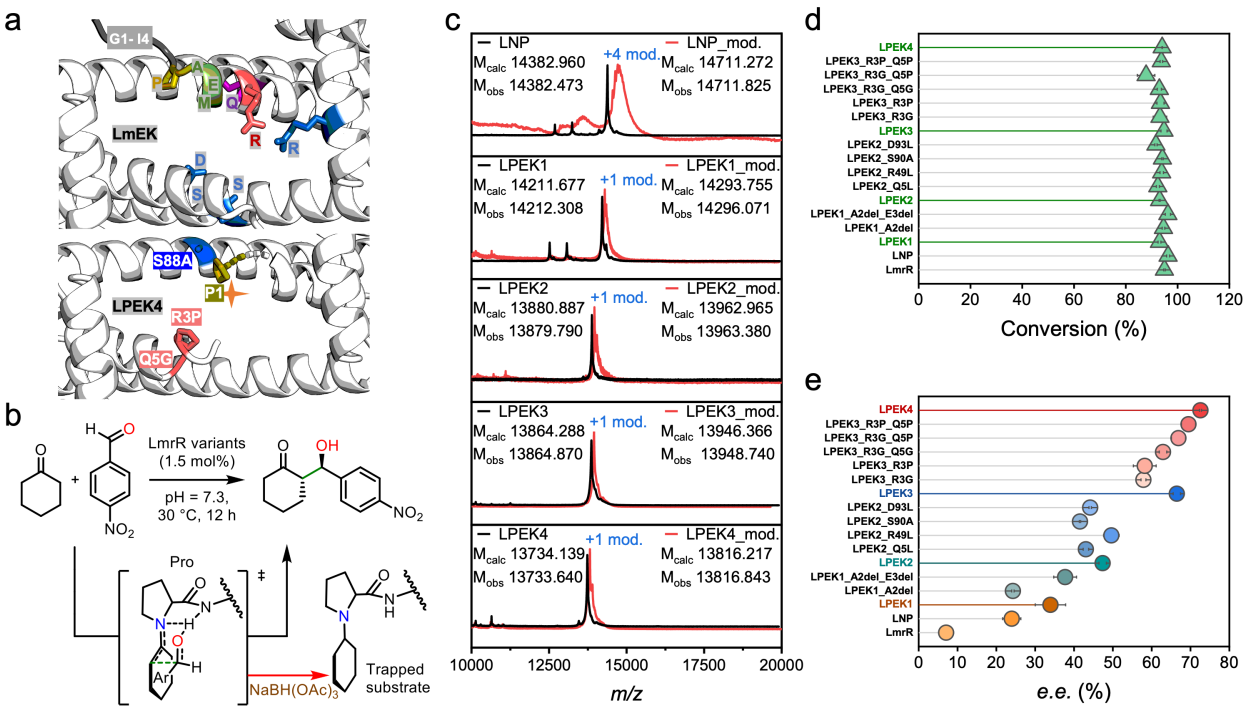

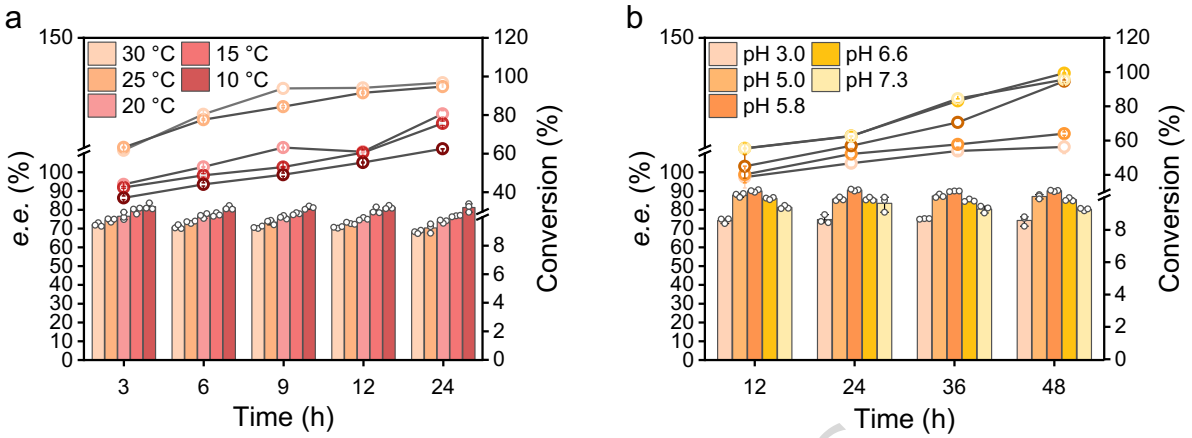

c

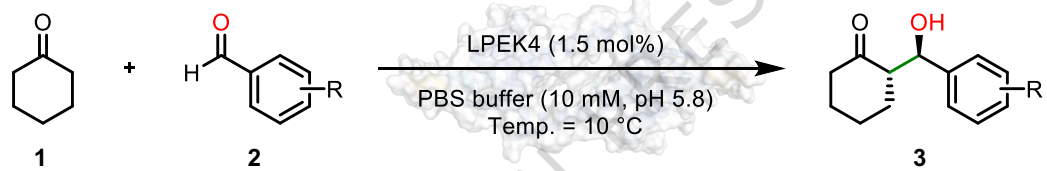

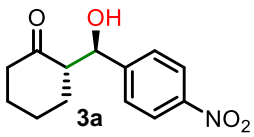

3a

Conv. = 94.7±0.6%
e.e. = 90.1±0.4%
d.r. = 87:13

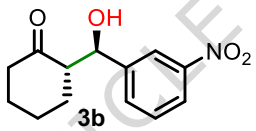

3b

Conv. = 93.3±3.0%
e.e. = 71.3±1.3%
d.r. = 74:26

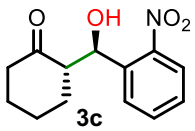

3c

Conv. = 91.7±2.0%
e.e. = 69.2±1.4%
d.r. = 68:32

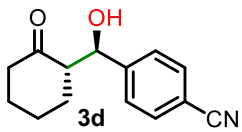

3d

Conv. = 91.5±0.3%
e.e. = 90.6±0.2%
d.r. = 91:9

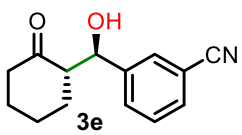

3e

Conv. = 91.8±0.9%
e.e. = 85.5±1.8%
d.r. = 83:17

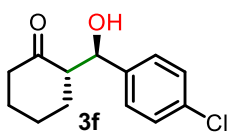

3f

Conv. = 99.0±0.1%
e.e. = 90.0±0.8%
d.r. = 84:16

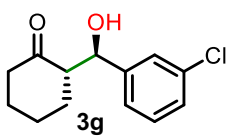

3g

Conv. = 93.9±2.1%
e.e. = 73.9±0.4%
d.r. = 79:21

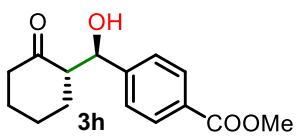

3h

Conv. = 92.8±1.9%
e.e. > 99%
d.r. = 94:6

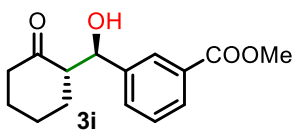

3i

Conv. = 89.1±2.3%
e.e. = 82.2±3.1%
d.r. = 82:18

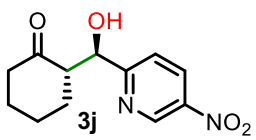

3j

Conv. = 76.7±1.4%
e.e. = 80.8±0.5%
d.r. = 74:26

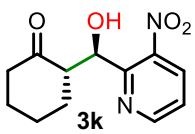

3k

Conv. = 76.7±1.0%
e.e. = 90.9±1.3%
d.r. = 79:21

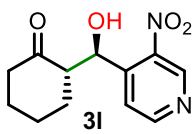

3l

Conv. = 80.5±2.3%
e.e. = 75.6±0.7%
d.r. = 75:25